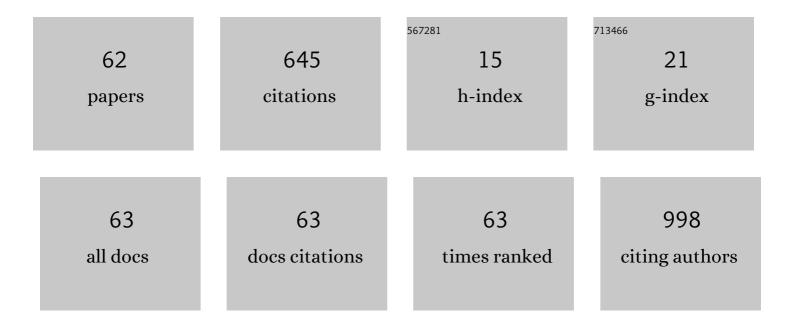
## Jinhee Jang

List of Publications by Year in descending order

Source: https://exaly.com/author-pdf/4017006/publications.pdf Version: 2024-02-01



#	Article	IF	CITATIONS
1	DIFFnet: Diffusion Parameter Mapping Network Generalized for Input Diffusion Gradient Schemes and b-Value. IEEE Transactions on Medical Imaging, 2022, 41, 491-499.	8.9	9
2	Editorial comment: Prognostic value of diffusion-weighted imaging in patients with newly diagnosed sporadic Creutzfeldt-Jakob disease. European Radiology, 2022, 32, 1939-1940.	4.5	0
3	Magnetic Resonance Imaging-Based Radiomics for the Prediction of Progression-Free Survival in Patients with Nasopharyngeal Carcinoma: A Systematic Review and Meta-Analysis. Cancers, 2022, 14, 653.	3.7	9
4	Low-Dose Three-Dimensional Rotational Angiography for Evaluating Intracranial Aneurysms: Analysis of Image Quality and Radiation Dose. Korean Journal of Radiology, 2022, 23, 256.	3.4	3
5	The Global Reading Room: Imaging After a Seizure. American Journal of Roentgenology, 2022, , .	2.2	1
6	Acute Ischemic Stroke caused by Internal Carotid Artery Occlusion: Impact of Occlusion Type on the Prognosis. World Neurosurgery, 2022, , .	1.3	0
7	Brain Iron Imaging in Aging and Cognitive Disorders: MRI Approaches. Journal of the Korean Society of Radiology, 2022, 83, 527.	0.2	0
8	Clinical Implications of Focal Mineral Deposition in the Globus Pallidus on CT and Quantitative Susceptibility Mapping of MRI. Korean Journal of Radiology, 2022, 23, 742.	3.4	4
9	Volumetric Measurement of Relative CBV Using T1-Perfusion-Weighted MRI with High Temporal Resolution Compared with Traditional T2*-Perfusion-Weighted MRI in Postoperative Patients with High-Grade Gliomas. American Journal of Neuroradiology, 2022, 43, 864-871.	2.4	1
10	Radiomics may increase the prognostic value for survival in glioblastoma patients when combined with conventional clinical and genetic prognostic models. European Radiology, 2021, 31, 2084-2093.	4.5	25
11	Identification of the intraparotid facial nerve on MRI: a systematic review and meta-analysis. European Radiology, 2021, 31, 629-639.	4.5	4
12	Low-Dose 3D Rotational Angiography in Measuring the Size of Intracranial Aneurysm: In Vitro Feasibility Study Using Aneurysm Phantom. Neurointervention, 2021, 16, 59-63.	0.8	3
13	Paradoxical paramagnetic calcifications in the globus pallidus: An ex vivo MR investigation and histological validation study. NMR in Biomedicine, 2021, 34, e4571.	2.8	5
14	Adverse effects of hypertension, supine hypertension, and perivascular space on cognition and motor function in PD. Npj Parkinson's Disease, 2021, 7, 69.	5.3	15
15	Intraindividual Comparison between the Contrast-Enhanced Golden-Angle Radial Sparse Parallel Sequence and the Conventional Fat-Suppressed Contrast-Enhanced T1-Weighted Spin-Echo Sequence for Head and Neck MRI. American Journal of Neuroradiology, 2021, 42, 2009-2015.	2.4	2
16	χ-separation: Magnetic susceptibility source separation toward iron and myelin mapping in the brain. NeuroImage, 2021, 240, 118371.	4.2	46
17	Optic Neuropathy Caused by an Ethmoid Sinus Mucocele Encasing the Optic Nerve. Neurology India, 2021, 69, 1125.	0.4	0
18	Preoperative assessment of cervical lymph node metastases in patients with papillary thyroid carcinoma: Incremental diagnostic value of dual-energy CT combined with ultrasound. PLoS ONE, 2021, 16. e0261233.	2.5	6

JINHEE JANG

#	Article	IF	CITATIONS
19	Cerebellar artery arising from the cavernous segment of the internal carotid artery and persistent trigeminal artery: a spectrum of incomplete longitudinal fusion. Acta Radiologica, 2020, 61, 386-394.	1.1	Ο
20	Estimating age-related changes in inÂvivo cerebral magnetic resonance angiography using convolutional neural network. Neurobiology of Aging, 2020, 87, 125-131.	3.1	8
21	A diffuse large B cell lymphoma with clinical, imaging, and serologic characteristics of neuromyelitis optica spectrum disorder. Leukemia and Lymphoma, 2020, 61, 999-1001.	1.3	1
22	The association between total lymphocyte count after concomitant chemoradiation and overall survival in patients with newly diagnosed glioblastoma. Journal of Clinical Neuroscience, 2020, 71, 21-25.	1.5	15
23	<scp>MRI</scp> â€visible dilated perivascular spaces in healthy young adults: A twin heritability study. Human Brain Mapping, 2020, 41, 5313-5324.	3.6	14
24	MRI and Quantitative Magnetic Susceptibility Maps of the Brain after Serial Administration of Gadobutrol: A Longitudinal Follow-up Study. Radiology, 2020, 297, 143-150.	7.3	15
25	Prediction of Human Papillomavirus Status and Overall Survival in Patients with Untreated Oropharyngeal Squamous Cell Carcinoma: Development and Validation of CT-Based Radiomics. American Journal of Neuroradiology, 2020, 41, 1897-1904.	2.4	14
26	Prognostic value of computed tomographyâ€based volumetric body composition analysis in patients with head and neck cancer: Feasibility study. Head and Neck, 2020, 42, 2614-2625.	2.0	9
27	Multiphasic Computed Tomography Angiography Findings for Identifying Pseudo-Occlusion of the Internal Carotid Artery. Stroke, 2020, 51, 2558-2562.	2.0	14
28	Dual-energy CT for differentiating acute intracranial hemorrhage from contrast staining or calcification: a meta-analysis. Neuroradiology, 2020, 62, 1617-1626.	2.2	22
29	Compressive Optic Neuropathy with a Concurrent Mutation of Leber's Hereditary Optic Neuropathy: A Case Report. Neuro-Ophthalmology, 2020, 44, 387-390.	1.0	1
30	IDH1 mutation prediction using MR-based radiomics in glioblastoma: comparison between manual and fully automated deep learning-based approach of tumor segmentation. European Journal of Radiology, 2020, 128, 109031.	2.6	20
31	Artificial Intelligence in Health Care: Current Applications and Issues. Journal of Korean Medical Science, 2020, 35, e379.	2.5	46
32	Paramagnetic Rims in Multiple Sclerosis and Neuromyelitis Optica Spectrum Disorder: A Quantitative		

JINHEE JANG

#	Article	IF	CITATIONS
37	Prognostic value of phase information of 2D T2*-weighted gradient echo brain imaging in cardiac arrest survivors: A preliminary study. Resuscitation, 2019, 140, 142-149.	3.0	18
38	Diagnostic accuracy and efficiency of combined acquisition of low-dose time-resolved and single-phase high-resolution contrast-enhanced magnetic resonance angiography in a single session for pre-angiographic evaluation of spinal vascular disease. PLoS ONE, 2019, 14, e0214289.	2.5	6
39	Dataâ€driven synthetic MRI FLAIR artifact correction via deep neural network. Journal of Magnetic Resonance Imaging, 2019, 50, 1413-1423.	3.4	16
40	Comparison of efficacy and complications between radiofrequency ablation and repeat surgery in the treatment of locally recurrent thyroid cancers: a single-center propensity score matching study. International Journal of Hyperthermia, 2019, 36, 358-366.	2.5	39
41	Relationship between Abnormal Hyperintensity on T2-Weighted Images Around Developmental Venous Anomalies and Magnetic Susceptibility of Their Collecting Veins: <i>In-Vivo</i> Quantitative Susceptibility Mapping Study. Korean Journal of Radiology, 2019, 20, 662.	3.4	3
42	Image Quality of Low-Dose Cerebral Angiography and Effectiveness of Clinical Implementation on Diagnostic and Neurointerventional Procedures for Intracranial Aneurysms. American Journal of Neuroradiology, 2019, 40, 827-833.	2.4	6
43	Quantitative analysis of relative volume of low apparent diffusion coefficient value can predict neurologic outcome after cardiac arrest. Resuscitation, 2018, 126, 36-42.	3.0	29
44	Deep gray matter iron measurement in patients with liver cirrhosis using quantitative susceptibility mapping: Relationship with pallidal T <sub>1</sub> hyperintensity. Journal of Magnetic Resonance Imaging, 2018, 47, 1342-1349.	3.4	10
45	Associations between Morphological Characteristics of Intracranial Arteries and Atherosclerosis Risk Factors in Subjects with Less Than 50% Intracranial Arterial Stenosis. Investigative Magnetic Resonance Imaging, 2018, 22, 150.	0.4	3
46	Correlation-based perfusion mapping using time-resolved MR angiography: A feasibility study for patients with suspicions of steno-occlusive craniocervical arteries. European Radiology, 2018, 28, 4890-4899.	4.5	0
47	Zuckerkandl Tubercle of the Thyroid Gland: Correlations between Findings of Anatomic Dissections and CT Imaging. American Journal of Neuroradiology, 2017, 38, 1416-1420.	2.4	11
48	Linear sign in cystic brain lesions ≥5 mm: A suggestive feature of perivascular space. European Radiology, 2017, 27, 4747-4755.	4.5	6
49	Assessment of Arterial Wall Enhancement for Differentiation of Parent Artery Disease from Small Artery Disease: Comparison between Histogram Analysis and Visual Analysis on 3-Dimensional Contrast-Enhanced T1-Weighted Turbo Spin Echo MR Images at 3T. Korean Journal of Radiology, 2017, 18, 383.	3.4	7
50	Diagnosis of Nerve Root Compromise of the Lumbar Spine: Evaluation of the Performance of Three-dimensional Isotropic T2-weighted Turbo Spin-Echo SPACE Sequence at 3T. Korean Journal of Radiology, 2017, 18, 249.	3.4	13
51	The Importance of Interface Irregularity between the Tumor and Brain Parenchyma in Differentiating between Typical and Atypical Meningiomas: Correlation with Pathology. Investigative Magnetic Resonance Imaging, 2016, 20, 158.	0.4	3
52	Radiation Doses of Various CT Protocols: a Multicenter Longitudinal Observation Study. Journal of Korean Medical Science, 2016, 31, S24.	2.5	8
53	The usefulness of diffusionâ€weighted readoutâ€segmented <scp>EPI</scp> and fast spin echo with <scp>BLADE</scp> ( <scp>PROPELLER</scp> ) kâ€space sampling: A comparison with singleâ€shot <scp>EPI</scp> for diffusionâ€weighted imaging in ischemic stroke patients. International Journal of Imaging Systems and Technology. 2016. 26. 216-224.	4.1	2
54	Progression of Vertebral Artery Dissection: Vessel Wall Enhancement and Aneurysm Dilation. Canadian Journal of Neurological Sciences, 2016, 43, 715-716.	0.5	2

JINHEE JANG

#	Article	IF	CITATIONS
55	The phase value of putamen measured by susceptibility weighted images in Parkinson's disease and in other forms of Parkinsonism: a correlation study with F18 FP-CIT PET. Acta Radiologica, 2016, 57, 852-860.	1.1	3
56	Detection of Leptomeningeal Metastasis by Contrast-Enhanced 3D T1-SPACE: Comparison with 2D FLAIR and Contrast-Enhanced 2D T1-Weighted Images. PLoS ONE, 2016, 11, e0163081.	2.5	18
57	Subtraction MR Venography Acquired from Time-Resolved Contrast-Enhanced MR Angiography: Comparison with Phase-Contrast MR Venography and Single-Phase Contrast-Enhanced MR Venography. Korean Journal of Radiology, 2015, 16, 1353.	3.4	5
58	Supra-aortic low-dose contrast-enhanced time-resolved magnetic resonance (MR) angiography at 3 T: comparison with time-of-flight MR angiography and high-resolution contrast-enhanced MR angiography. Acta Radiologica, 2015, 56, 673-680.	1.1	6
59	Bilateral Thalamic Infarction After Traumatic Vertebral Artery Dissection. Canadian Journal of Neurological Sciences, 2015, 42, 208-209.	0.5	2
60	Non-stenotic intracranial arteries have atherosclerotic changes in acute ischemic stroke patients: a 3T MRI study. Neuroradiology, 2015, 57, 1007-1013.	2.2	17
61	Non-contrast-enhanced 4D MR angiography with STAR spin labeling and variable flip angle sampling: a feasibility study for the assessment of Dural Arteriovenous Fistula. Neuroradiology, 2014, 56, 305-314.	2.2	22
62	Reflux venous flow in dural sinus and internal jugular vein on 3D time-of-flight MR angiography. Neuroradiology, 2013, 55, 1205-1211.	2.2	24